Received 20 February 2023; revised 12 May 2023; accepted 24 May 2023. Date of publication 2 June 2023;
date of current version 20 June 2023. Recommended by Senior Editor Fabio Pasqualetti.

Digital Object Identifier 10.1109/OJCSYS.2023.3282438

Dual Control of Coupled Oscillator Networks

PER SEBASTIAN SKARDAL [1] AND ALEX ARENAS [2]

(Synchronization in Natural and Engineering Systems)

[1]Department of Mathematics, Trinity College, Hartford, CT 06106 USA
[2]Departament d'Enginyeria Informatica i Matemátiques, Universitat Rovira i Virgili, 43007 Tarragona, Spain

CORRESPONDING AUTHOR: PER SEBASTIAN SKARDAL (e-mail: persebastian.skardal@trincoll.edu)

The work of Per Sebastian Skardal was supported by the NSF under Grant MCB-2126177. The work of Alex Arenas was supported in part by the Joint Appointment Program, Pacific Northwest National Laboratory, a multi-program national laboratory operated for the U.S. Department of Energy (DOE) by Battelle Memorial Institute under Grant DE-AC05-76RL01830, in part by Spanish MICINN under Grant PID2021-128005NB-C21, in part by the European Union's Horizon Europe Programme under the CREXDATA project, under Grant 101092749, in part by Generalitat de Catalunya under Grant 2017SGR-896, in part by Universitat Rovira i Virgili under Grant 2021SGR-00633, in part by ICREA Academia 2023, and in part by the James S. McDonnell Foundation under Grant 220020325.

ABSTRACT Robust coordination and organization in large ensembles of nonlinear oscillatory units play a vital role in a wide range of natural and engineered system. The control of self-organizing network-coupled systems has recently seen significant attention, but largely in the context of modifying or augmenting existing structures. This leaves a gap in our understanding of reactive control, where and how to design direct interventions, and what we may learn about structure and dynamics from such control strategies. Here we study reactive control of coupled oscillator networks and demonstrate dual control strategies, i.e., two different mechanisms for control, that may each be implemented on their own and interchangeably to achieve synchronization. These diverse strategies exploit different network properties, with the first directly targeting oscillators that are challenging to entrain, and the second focusing on oscillators with a strong influence on others. Thus, in addition to presenting alternative strategies for network control, the distinct control sets illuminate the oscillators' dynamical and structural roles within the system. The applicability of dual control is demonstrated using both synthetic and real networks.

INDEX TERMS Complex networks, control, synchronization.

I. INTRODUCTION

A key benchmark for human scientific endeavor is to understand, control, and optimize the natural and man-made complex systems around us. A special challenge emerges in the context of coordinating large, network-coupled ensembles of oscillators [1], [2], [3]. Besides exhibiting immense complexity, self-organization of such systems underpins critical function in a wide range of applications such as cellular circuits, cardiac pacemakers, and power grids [4], [5], [6]. On the one hand, the control of network dynamics, both linear and nonlinear, has seen significant attention in recent years [7], [8], [9], [10], [11], [12], [13], [14], [15], [16], with attention to control and optimization of oscillator systems specifically focusing largely on the design of the underlying network structure [17], [18], [19], [20], [21], [22], [23]. On the other hand, the more direct approaches of reactive and pinning control, which directly intervene in the system dynamics at chosen nodes [24], [25], [26], [27], have been explored to a lesser degree, leaving an incomplete understanding of precisely where and how to intervene in self-organizing systems to exert control. Moreover, the extent to which we may gain insight into a network's structure and/or dynamics from control implementation remains largely unclear.

In this paper, we investigate the reactive control of heterogeneous oscillator networks. We highlight that the control strategy utilized here falls into the category of reactive control that generalizes pinning control. Specifically, while pinning control typically aims to achieve perfect homogeneity through pinning to a uniform state, we strive to achieve a target state that is heterogeneous, thus necessitating varied controllers. We demonstrate that there are dual control strategies targeting different sets of oscillators that may be conveniently and interchangeably used to achieve a controlled, synchronized state. Besides providing two distinct options for controlling

network dynamics, these strategies shed light on different roles of oscillators in the networks. The first strategy, which we'll refer to as 'row control' due to the mathematics underlying its derivation, directly exerts control, identifying those oscillators that tend not to entrain with the rest of the network independently. The second strategy, dubbed 'column control', acts more indirectly, targeting oscillators that do not necessarily require entrainment themselves, but rather exert a strong influence on other oscillators, thus playing a pivotal role in entraining the complete system. Utilizing both synthetic and real network topologies, we demonstrate the applicability and efficacy of both control strategies.

We also examine the properties of the sets of oscillators requiring control via the two different strategies as the overall network coupling varies, namely, the row control set and column control set. Intriguingly, as the generic properties of oscillators belonging to the 'column control set' remain largely unaffected by overall coupling, the coupling induces a transition in the properties of oscillators belonging to the 'row control set'. Specifically, when overall coupling is small, yielding strongly disordered uncontrolled dynamics, the oscillators needing direct control resemble hubs with many incoming connections. Conversely, when overall coupling is large, leading to less disorder in the uncontrolled dynamics, the oscillators needing direct control have relatively few incoming connections.

II. COUPLED OSCILLATOR NETWORKS AND CONTROL

In this work we consider network-coupled systems of N Kuramoto oscillators [28] whose dynamics are governed by

$$\dot{\theta}_i = \omega_i + K\sum_{j=1}^{N} A_{ij}\sin(\theta_j - \theta_i) + f_i(t), \tag{1}$$

where θ_i and ω_i are the phase and natural frequency of oscillator i, K is the global coupling strength, and the adjacency matrix A encodes the structure of the underlying network, which we assume is directed, and lastly the function $f_i(t)$ represents the possible reactive control exerted onto oscillator i. (The choice $f_i(t) = 0$ corresponds to no control imposed at all.) Here we focus on the unweighted directed case, where $A_{ij} = 1$ if a link $j \to i$ exists and $A_{ij} = 0$ otherwise, but our results generalize to weighted links. We focus on the (complete) synchronization of the ensemble of oscillators, i.e., we target the state where they all process with the same angular velocity,

$$\lim_{t\to\infty} |\dot{\theta}_i(t) - \dot{\theta}_j(t)| = 0 \quad \text{for all} \quad i, j = 1, \ldots, N. \tag{2}$$

It should also be noted that a common metric for the degree of synchronization in a network is Kuramoto's order parameter, given by $z = re^{i\psi} = N^{-1}\sum_{j=1}^{N} e^{i\theta_j}$, whose amplitude r delineates weakly and strongly clustered states ($|z| \approx 0$ and $|z| \sim 1$, respectively). We note, that the value of the order parameter may not easily be used to identify complete synchronization, but its asymptotic behavior may, with a completely synchronized state yielding relaxation to a fixed value, i.e., $|z(t)| \to r_\infty$ as $t \to \infty$.

A. TARGET STATE AND STABILITY

Our control mechanisms begins by identifying a target, synchronized state. Specifically, we seek a target state of the form $\boldsymbol{\theta}^{\text{target}}(t) = \boldsymbol{\theta}^* + \boldsymbol{\Omega}t$, where $\boldsymbol{\theta}^* \in \mathbb{R}^N$ is a static vector of heterogeneous values and $\boldsymbol{\Omega} \in \mathbb{R}^N$ is the constant vector whose values Ω are given by the collective frequency of the synchronized system. We proceed by linearizing (1) to obtain, in vector form,

$$\dot{\boldsymbol{\theta}} = \boldsymbol{\omega} - KL\boldsymbol{\theta}, \tag{3}$$

where L is the Laplacian matrix whose entries are given by $L_{ij} = \sum_{l=1}^{N} A_{il}$ if $i = j$ and $L_{ij} = -A_{ij}$ otherwise. Inserting the target state into (3) yields

$$\boldsymbol{\theta}^* = K^{-1}L^{\dagger}(\boldsymbol{\omega} - \boldsymbol{\Omega}), \tag{4}$$

where $L^{\dagger}$ is the pseudoinverse of L [29]. Moreover, it can be shown that the collective frequency Ω is, in general, not equal to the mean natural frequency, but in the general case of a directed network, equal to a weighted average of the natural frequencies, where the weights come from the first left singular vector $\boldsymbol{u}^1$ of L, i.e., $\Omega = \langle \boldsymbol{u}^1, \boldsymbol{\omega}\rangle / \langle \boldsymbol{u}^1, \mathbf{1}\rangle$ [30], [31].

With our synchronized target state in hand, we now seek to control the network dynamics by ensuring its stability. We choose a controller that aims to achieve a heterogeneous state encoded in $\boldsymbol{\theta}^*$, specifically $f_i(t) = F_i \sin(\theta_i^{\text{target}}(t) - \theta_i(t))$ for oscillator i, where F_i is the control strength and $\theta_i^{\text{target}}(t) = \theta_i^* + \Omega t$. Note that (i) the sine function is chosen since the dynamics evolve on the torus and (ii) the heterogeneous nature of controllers (which stems from the heterogeneity of $\boldsymbol{\theta}^*$) differentiates this method from typical pinning control. We will then aim to achieve control by stabilizing the target state, whose Jacobian is given by

$$DF_{ij}|_{\boldsymbol{\theta}=\boldsymbol{\theta}^*} = \begin{cases} -K\sum_{j\neq i} w_{ij} - F_i & \text{if } i = j \\ K w_{ij} & \text{if } i \neq j \end{cases} \tag{5}$$

where $w_{ij} = A_{ij}c_{ij}$ and $c_{ij} = \cos(\theta_j^* - \theta_i^*)$. Stability of the target state, and thereby control of the synchronized state, is achieved by ensuring that the full spectrum of eigenvalues lies in the left-half complex plane. We note that, in the uncontrolled case (where $F_i = 0$) the rows of the Jacobian sum to zero, yielding at least one trivial eigenvalue $\lambda_1 = 0$, corresponding to a marginal stability induced by rotational symmetry, so we seek to ensure that the real part of all eigenvalues are non-positive.

B. ROW AND COLUMN CONTROL

Our two different control strategies stem from the application of the Gershgorin circle theorem [32], which can be applied to either the rows or the columns of DF. Following [27], application of the theorem to the rows ensures that all N eigenvalues lie within the union of N row discs, $\bigcup D_i^{\text{row}}$,

TABLE 1. Summary of control conditions and required gain for row and column control strategies.

row control	column control
control i if $\exists\ j$ with $w_{ij} < 0$	control j if $\sum_{i\neq j} \lvert w_{ij}\rvert > \sum_{i\neq j} w_{ji}$
gain: $F_i \geq K \sum_{j\neq i} (\lvert w_{ij}\rvert - w_{ij})$	gain: $F_j \geq K \sum_{i\neq j} (\lvert w_{ij}\rvert - w_{ji})$

where the i^{th} disc D_i^{row} is centered at DF_{ii} and has radius $\sum_{j\neq i} |DF_{ij}|$. Beginning with no control, i.e., $F_i = 0$, the i^{th} discs is centered at $DF_{ii} = -K\sum_{j\neq i} w_{ij}$ and has a radius $r_i = K\sum_{j\neq i} |w_{ij}|$. This disc contains some portion in the right half complex plane, thereby admitting the possibility of an eigenvalue with positive real part, if any w_{ij} in row i is negative. Thus, by inspecting the rows of DF we identify all oscillators that require control and for those oscillators set $F_i \geq K\sum_{j\neq i}(|w_{ij}| - w_{ij})$. We refer to this strategy as *row control*.

Our second strategy, which we refer to as *column control*, stems from applying the Gershgorin circle theorem to the columns of DF. From this perspective the eigenvalues lie within the union of column discs, $\bigcup D_j^{\text{column}}$, where D_j^{column} is centered at $DF_{jj} = -K\sum_{i\neq j} w_{ji}$ and has radius $\sum_{i\neq j} |DF_{ij}| = K\sum_{i\neq j} |w_{ij}|$. It follows that oscillator j requires column control if it satisfies $\sum_{i\neq j} |w_{ij}| > \sum_{i\neq j} w_{ji}$, and for each we set $F_j \geq \sum_{i\neq j}(|w_{ij}| - w_{ji})$. In Table 1 we summarize the condition for an oscillator (i or j) needing row or column control (top row) and the required control gain for each such oscillator (bottom row).

C. PRACTICAL CONSIDERATIONS

Before proceeding to examples of the applicability of dual control of oscillator networks, we make a few remarks about practical considerations. In particular, we note that the theoretical underpinning of both row and column control relies on the linearization of (1) to obtain (3). This linearization is of course an approximation whose accuracy may vary depending on various properties of the system, namely the network topology, natural frequencies, and coupling strength. Thus, sufficient loss of accuracy may lead to failure of the control method unless certain precautions are taken. In particular, we find that two particular practical steps may be taken to improve the success of the control mechanism.

The first practical step we take is to adjust the target state to better represent a target state obtained by solving the nonlinear system (i.e., one involving arcsines). For this we introduce a parameter ϵ_K which we use to modify the target state, specifically to use the target state

$$\boldsymbol{\theta}^* = \frac{L^\dagger(\boldsymbol{\omega} - \boldsymbol{\Omega})}{K(1-\epsilon_K)}. \tag{6}$$

Here we assume that ϵ_K is positive and relatively small, so that the target state is slightly expanded, i.e., more spread out, than without ϵ_K. For the examples below we use $\epsilon_K = 0.2$.

The second practical step we take is to add a margin of error in our identification of control oscillators depending on the rows/columns of the Jacobian. Ultimately, we seek to err on the conservative side and rather add a handful of addition oscillators to the control sets to overcome inaccuracies from approximations. For this purpose, we introduce a parameter ϵ_{DF} that is applied slightly differently in the row and column control strategies. For row control, rather than identifying entries of DF where a link $j \to i$ exists and $DF_{ij} < 0$, we allow for some margin of error by controlling oscillator i if row i contains an entry for which $j \to i$ and $DF_{ij} < \epsilon_{DF}$. For column control, we simply imposecontrol on oscillator j if the j^{th} Gershgorin disc is within ϵ_{DF} of the right-side complex plane. Similar to ϵ_K, we assume that ϵ_{DF} is positive and relatively small, so that some additional margin of error is given to ensure that eigenvalues of the Jacobian are pushed into the left half complex plane. In the main text we use $\epsilon_{DF} = 0.2$.

III. ILLUSTRATIVE EXAMPLES

Next we examine some illustrative examples of row and column control. We begin by considering a small, synthetic directed network, then turn our attention to a real power grid network that is undirected but effectively becomes directed when parameter heterogeneity is incorporated.

A. EXAMPLE USING A SYNTHETIC NETWORK

In our first example we demonstrate row and column control using a small network of $N = 12$ nodes with average degree $\langle k\rangle = 2$, whose topology is illustrated in Fig. 1(a). Moreover, natural frequencies are randomly generated and denoted in parentheses, and the coupling strength is set to $K = 1.22$. For this set of parameters we identify the sets of row (blue) and column (red) controlled oscillators, which consist of three and four oscillators, respectively. Note that these sets are very different, only overlapping at a single oscillator (shaded both blue and red). In Fig. 1(b) and (c) we plot the time series for the phases $\theta_i(t)$ for row and column control, respectively. In particular, starting from the same initial conditions we allow the systems to evolve without control initially, for $t < 0$, then turn on the respective control mechanism at $t = 0$, letting systems then evolve with control for $t > 0$. As the control sets differ, so do the the dynamics of the phases, most notably just after control is turned on, but both relax to completely synchronized states. In fact, steady-state of the two cases also differ, which can be most easily identified in the time series of order parameters in Fig. 1(d). We emphasize that, despite the significant disorder in the phases' dynamics without control and the significant difference between the row and column control sets, both strategies are effectively synchronize the system dynamics. Below we examine in greater detail the properties of the control sets, namely the properties of oscillators in the row and column control sets, as well as their respective sizes and overlap.

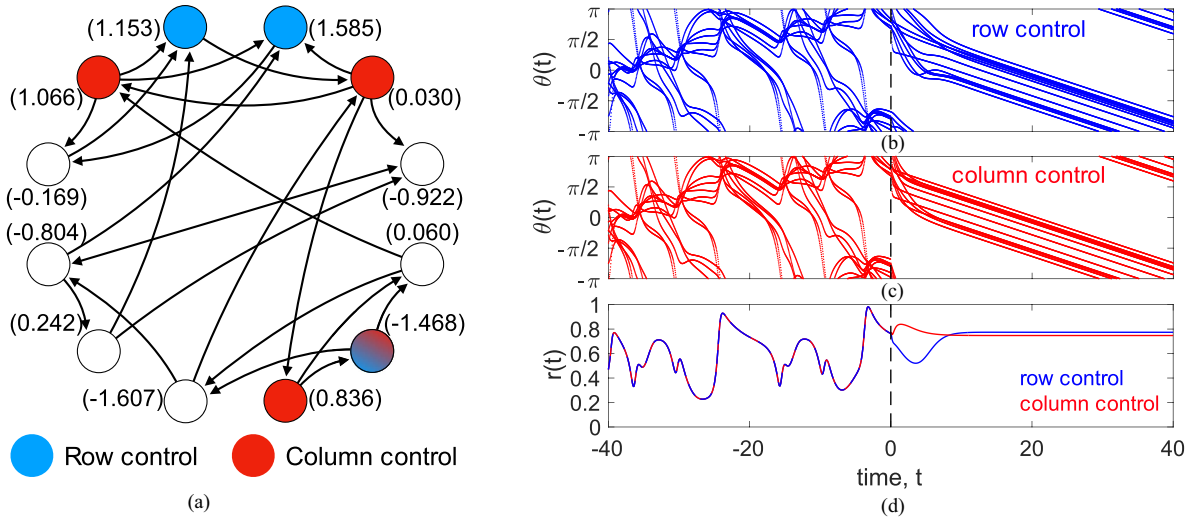

FIGURE 1. Dual control strategies for complex oscillator networks. (a) A 12-node directed network with average degree $\langle k \rangle = 2$. Natural frequencies are indicated in parentheses, the coupling strength is $K = 1.22$, and row- and column-controlled oscillators are filled blue and red, respectively. Time series for collection of phases under (b) row control, (c) column control, and (d) the magnitude of the order parameter $r(t)$ before ($t < 0$) and after ($t \geq 0$) control is applied.

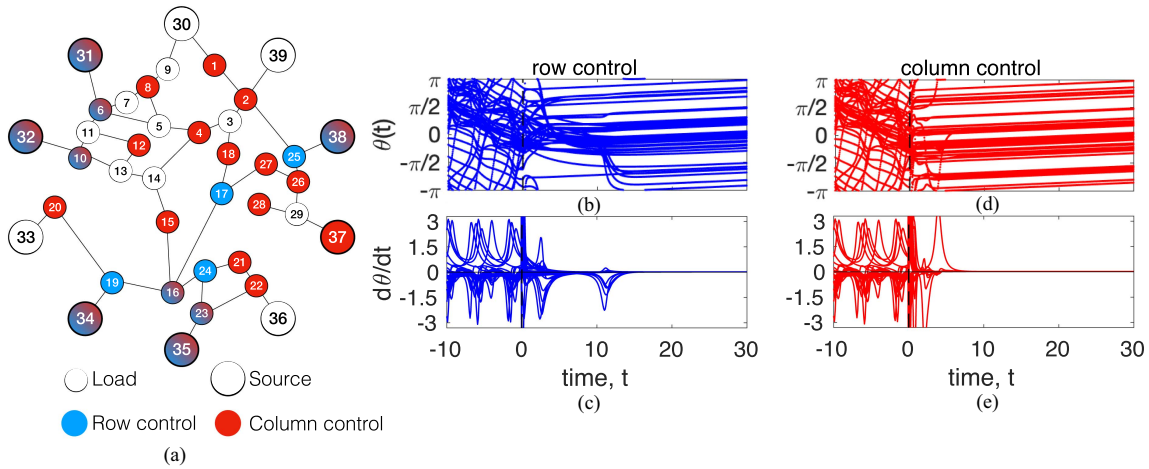

FIGURE 2. Dual control of the IEEE 39 New England power grid. (a) The 39-node IEEE New England power grid network, denoting loads and sources as small (inner) and large (outer) nodes. Natural frequencies and damping coefficients are provided in Appendix A. Row and column controlled oscillators are colored blue and red, respectively. Time series for collection of (b),(d) phases and (c),(e) frequencies are plotted before ($t < 0$) and after ($t \geq 0$) control is applied.

B. APPLICATION TO THE IEEE 39 NEW ENGLAND POWER GRID

Next, we present an example application using the IEEE 39 New England power grid network [34]. We use this opportunity to emphasize that, for row and column control to differ, the network structure needs to be directed, i.e., we need $A^T \neq A$. (If the network is in fact undirected, then row and column control simply are indistinguishable.) However, for different applications certain heterogeneities in system parameters may render a network that is structurally undirected effectively directed, resulting in the emergence of dual control. We emphasize here that first order Kuramoto systems serve as accurate models for a variety of types of power grids [36], [37], [38], [39] and we consider the IEEE 39 New England power grid network with the following oscillator model

$$D_i\dot{\phi}_i = p_i + K\sum_{j=1}^{N} a_{ij}\sin(\phi_j - \phi_i), \tag{7}$$

where, even for an undirected topology encoded in the entries a_{ij}, heterogeneity in the damping coefficients D_i yield an effectively directed adjacency matrix entries $A_{ij} = a_{ij}/D_i$, as well as effective natural frequencies given by the ratio of the power and damping, $\omega_i = p_i/D_i$. In Fig. 2(a) we illustrate the topology of the power grid, with small inner nodes corresponding to loads and large outer nodes corresponding to sources. Damping coefficients D_i and power p_i are chosen randomly, with power biased positive or negative for

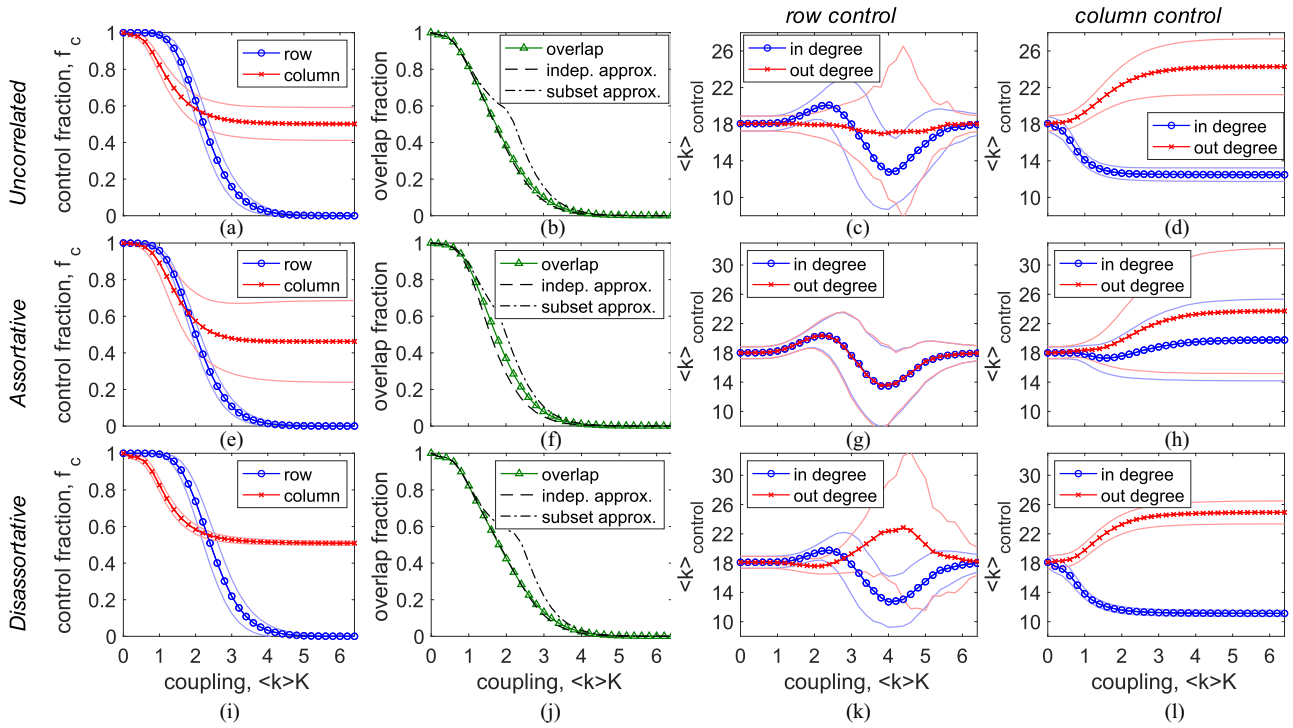

FIGURE 3. Network properties of row and column control. For an ensemble of 500 networks with $N = 200$ nodes, power-law exponent $\gamma = 3$, minimum degree $k_0 = 9$, and normally distributed natural frequencies, (a) the mean control fraction f_c for row (blue circles) and column control (red crosses) as a function of overal coupling, $\langle k \rangle K$, (b) the overlap fraction (green triangles) compared to independence and subset approximations (dashed and dot-dashed black curves). For the same ensemble of networks, the mean control in- and out-degrees $\langle k^{\text{in/out}} \rangle_{\text{control}}$ as a function of overall coupling (c) row and (d) column control. Standard deviations are indicated in (a), (c), and (d) using solid curves. The analogous results as those given in (a)–(d) are given in (e)–(h) and (i)–(l) for networks generated with, respectively, assortative and disassortative in- and out-degrees.

sources and loads, respectively. Power and damping parameters for each oscillator indexed in panel (a) are summarized in Appendix A. We then implement both row and column control, coloring row and column controlled oscillators blue and red, respectively, then plot the time series for the phases before ($t < 0$) and after ($t \geq 0$) control in panels (b) and (d). We also plot the time series of actual frequencies $d\theta/dt$ in panels (c) and (e). We observe that in this particular system there exists a trade-off in the efficacy of row vs column control. Namely, while column control synchronizes the system dynamics quicker than row control, row control requires direct control of fewer oscillators.

IV. CONTROL AND NETWORK STRUCTURE

Having demonstrated the application of dual control in the examples above, we now turn to study how row and column control depend on the network structure, the structural properties of oscillators the different control sets, and what row and column control reveal about the dynamical and structural roles of the oscillators in a network.

A. ROW VS COLUMN CONTROL SETS & OVERLAP

We begin by examining overall fraction of oscillators that require control under row and column control strategies, introducing the control fraction $f_c = n_c/N$, where n_c is the number of nodes that belong to the appropriate control set. We plot the control fraction f_c in Fig. 3(a) as a function of the overall coupling $\langle k \rangle K$ for row and column control in blue circles and red crosses, respectively. Results are taken from an ensemble of 500 networks of size $N = 200$ generated with the configuration model [33] with uncorrelated power-law in- and out-degree distributions with exponent $\gamma = 3$ and minimum degree $k_0 = 9$. For each network realization the natural frequencies are drawn from a standard normal distribution. Standard deviations of f_c are indicated by solid curves. While we observed in both examples above that the size of the column control set was larger than the row control set, these results reveal a more nuanced comparison between the two sets. In particular, the column control set indeed is larger than the row control set for sufficiently large coupling (here approximately $\langle k \rangle K > 2$), where row control tends is extremely efficient, however for smaller coupling there is a range (approximately $\langle k \rangle K < 2$) where column control is more efficient.

Next, to better understand how similar/dissimilar the row and column control sets are, we examine the overlap between thee two sets, which we plot in Fig. 3(b) in green triangles. Moreover, it's useful to compare these results to two approximations that stem from the two different hypotheses: (i) row and column control sets are largely independent or (ii) one set tends to be nearly contained within the other. Denoting these as the *independence* and *subset* approximations, respectively, the independence approximation would indicate that the overlap set is approximately the size of the product of

the row and column sets, where as the subset approximation would indicate that the overlap set is approximately equal to the minimum size of the row and column sets. Note that the latter case serves as an upper bound on any overlap set. Plotting the independence and subset approximations in dashed and dot-dashed black, we observe that the the independence approximation is the most accurate, indicating that row and column control largely target different oscillators in the network.

B. ROLE OF ROW & COLUMN CONTROL OSCILLATORS

Finally, we delve into a more detailed examination of the properties of the individual oscillators in the row and column control sets to better understand the dynamical and structural roles that these oscillator play in the network. To this end, we denote $\langle k^{\text{in/out}}\rangle_{\text{control}}$ as the mean in- or out-degree of oscillators in a given control set. In Fig. 3(c) and (d) we plot $\langle k^{\text{in}}\rangle_{\text{control}}$ and $\langle k^{\text{out}}\rangle_{\text{control}}$ (blue circle and red crosses, respectively) as a function of overall coupling $\langle k\rangle K$ for row and column control, respectively.

Starting with row control in panel (c), we observe that it is the in-degree of the oscillators in the row control set varies significantly depending on the coupling, while the out-degree of oscillators in the row control set varies very little. First, this is perhaps not surprising due to the application of the Gershgorin circle theorem along rows. However, the nature of how the in-degree varies as a function of coupling reveals a great deal about the nature of row control itself and the properties of the row control set. Namely, when the coupling is relatively small (say, $\langle k\rangle K \leq 3$) the oscillators that require control tend to have large in-degrees, whereas when the coupling is relatively large (say, $\langle k\rangle K \leq 3$), the oscillators that require control tend to have small in-degrees. Thus, when the uncontrolled dynamics are more disordered (smaller coupling) row control targets nodes with relatively higher degree, who are acted upon by relatively more destabilizing neighbors. On the other hand, when the uncontrolled dynamics are less disordered (larger coupling) row control targets nodes with relatively lower degree, who are acted upon by relatively few stabilizing neighbors. Thus, depending on the overall coupling the system itself acts as a destabilizing (more disorder) or stabilizing (less disorder) foundation, requiring row control to target oscillators with different properties.

Turning to column control in Fig. 3(d) the role of in- vs out-degrees is more apparent than the case of row control, as column-controlled oscillators tend to balance larger out-degrees with lower in-degrees. Mathematically this can be explained using the application of the Gershgorin circle theorem to the columns of DF: in the limit of strong coupling the target phases all take small values resulting the approximation $c_{ij} = \cos(\theta_j^* - \theta_i^*) \approx 1$, in which case the application of the Gershgorin circle theorem easily yields control for column j if $k_j^{\text{out}} > k_j^{\text{in}}$. Moreover, these local properties reveal the role played by oscillator in the column control set as influencers that have more out-going links than in-going links. Thus, column control achieves synchronization by a different strategy than row control: whereas row control directly targets oscillators that are difficult to entrain in various parameter regimes, column control achieves synchronization in a more indirect way, targeting oscillators that have a relatively strong influence throughout the network.

To further substantiate these results we consider networks with both assortative and disassortative mixing between nodal in- and out-degrees. For each case we again consider 500 networks of size $N = 200$ with the same parameters as above. However, to additionally attain positive or negative correlations, we simply match the largest in- degree with the largest or smallest out-degrees for assortative or disassortative networks, respectively, then to ensure some randomness, randomly swap the out-degrees of 2% of the assigned nodes. In Fig. 3 we plot the results for assortative (middle row) and disassortative networks (bottom row). We observe little change in the results for the control fraction f_c (Fig. 3(e) and (i)) and overlap fractions (Fig. 3(f) and (j)). Similarly, the mean degrees of the control sets support our previous explanation, specifically that membership of the row control set is largely dictated by in-degree and out-degree is negligible, and members of the column control set balance large out-degrees with small in-degrees.

Beyond investigating the role that network structure plays in row and column control for random network topologies, we also investigate the role of network structure in real world networks. With the application of power grid dynamics in mind, we consider two power grid networks: the IEEE 39 power grid used above and the RTS 96 power grid [35]. These networks are illustrated at the top left and right, respectively, in Fig. 4, with plots of the control fraction f_c, overlap fraction, and mean control in- and out-degrees $\langle k^{\text{in/out}}\rangle_{\text{control}}$ for row and column control as a function of overall coupling plotted in the left and right columns, panels (a)–(d) for the IEEE 39 power grid and panels (e)–(h) for the RTS 96 power grid. Results represent an average over 500 natural frequency realizations. Keeping with the application to power grids, nodes corresponding to sources and loads have natural frequencies drawn from normal distributions centered at -1 and 3, respectively, both with standard deviation 0.5. Sources and loads are identified as previously in the IEEE 39 power grid, while sources and loads are randomly chosen (25% of nodes are chosen to be sources) in the RTS power grid at each realization. The results observed for these real networks are similar to those for random network topologies except for the following. First, for both real networks the average row control fraction is always less than or equal to the column control fractions (Fig. 4(a) and (e)). While there are individual realization where the column control fraction is less, a range of coupling strengths where the column control fraction is prominently less than the row control fraction is not observed. The mean control in- and out-degrees for row control also behave differently (Fig. 4(c) and (g)). For the IEEE 39 power grid it first decreases as the coupling is increased, then increases before decreasing again to the mean degree, while for the RTS 96 power grid a meaningful relationship is difficult to observe. On the other

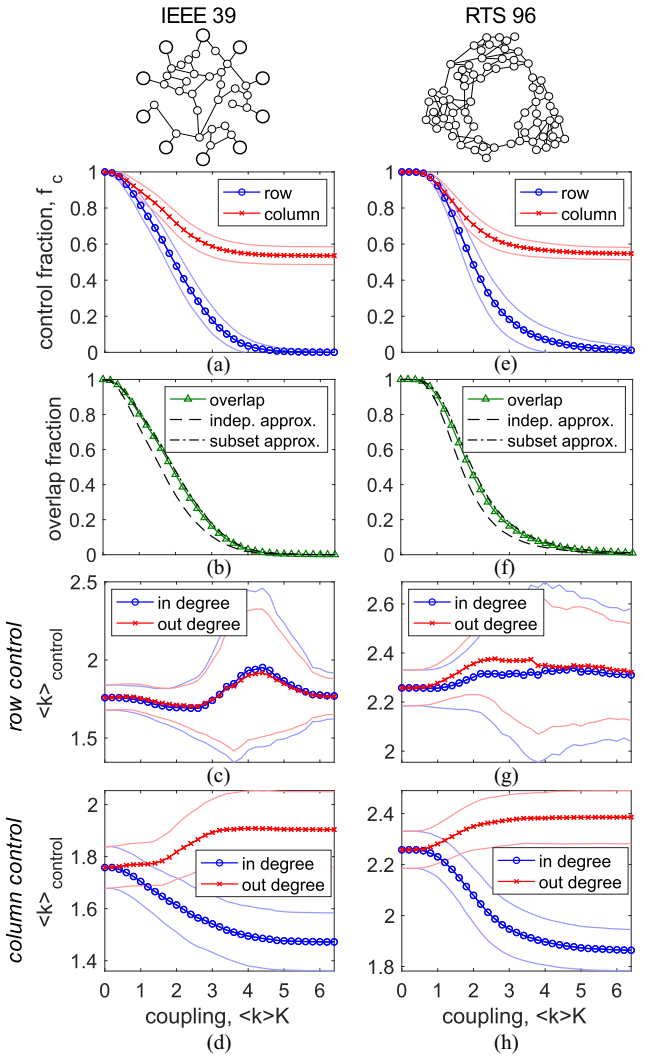

FIGURE 4. **Network properties of row and column control: real networks. The control fraction f_c, overlap fraction, and mean control in- and out-degrees $\langle k^{\text{in/out}}\rangle_{\text{control}}$ as functions of overall coupling $\langle k\rangle K$ for the IEEE 39 network, (a)–(d), and the RTS 96 network, (e)–(h). Results represent an average over 500 frequency realization. Network structures are illustrated at the top of the left and right columns.**

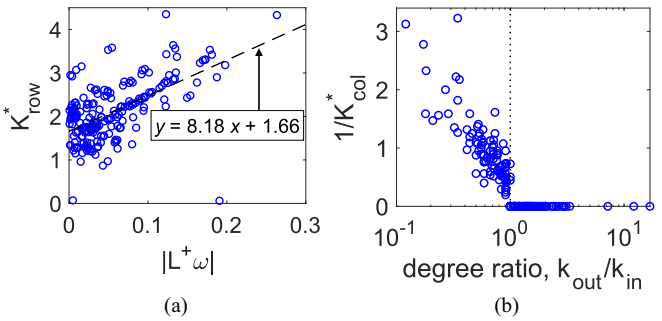

FIGURE 5. **Critical coupling strengths for row and column control. For an illustrative example of an $N = 200$ network with $\gamma = 9$, $k_0 = 9$, and normally distributed frequencies, (a) the nodal critical coupling strength for row control $K^*_{i,\text{row}}$ vs the scaled target state $|[L^\dagger\omega]_i|$, and (b) the inverse of the nodal critical coupling strength $1/K^*_{i,\text{col}}$ vs the degree ratio $k_i^{\text{out}}/k_i^{\text{in}}$.**

hand, the mean control in- and out-degrees for column control behave very similarly as the random network topologies, with control sets balancing larger ratios of out-to-in-degrees (Fig. 4(d) and (h)).

Lastly, we examine more closely the role of network structure and local dynamics in the makeup of the row and column control sets. To begin, we consider as a quantitative measure for the need of control for a given oscillator the quantity K_i^*, defined as the critical coupling value between which node i is and is not part of the control set. I.e., under row control, oscillator i is part of the row control set if $K < K^*_{i,\text{row}}$ but is not part of the row control set if $K > K^*_{i,\text{row}}$, and similarly for column control. I.e., larger (smaller) values of K_i^* indicate that oscillator i is more (less) in need of control. Beginning now with row control, returning to the basic condition of a row of the Jacobian having a negative off-diagonal entry and neglecting the collective frequency Ω, it follows that oscillator i needs control if it has a neighbor j satisfying $|\theta_j^* - \theta_i^*| = |[L^\dagger\boldsymbol{\omega}]_j/K - [L^\dagger\boldsymbol{\omega}]_i/K| > \pi/2$. Thus, oscillator i is more (less) likely to need control if its own value $[L^\dagger\boldsymbol{\omega}]_i$ is large (small). In Fig. 5(a) we plot the critical coupling value $K^*_{i,\text{row}}$ for each oscillator as a function of $[L^\dagger\boldsymbol{\omega}]_i$ for an illustrative example using a single network constructed using the same parameters as those used in Fig. 3(a)–(d). In fact, a strong positive relationship is observed between the two, fit best by the line $K^*_{i,\text{row}} \approx 1.66 + 8.18[L^\dagger\boldsymbol{\omega}]_i$.

For the case of column control, it is more useful to begin by considering the limit of large coupling, i.e., $K \gg 1$, for which that target state of each node i is given by $\theta_i^* = [L^\dagger\boldsymbol{\omega}]_i/K \ll 1$ and $\cos(\theta_j^* - \theta_i^*) \approx 1$. Thus, without any control the entries of the Jacobian are given by $DF_{ii} \approx -K\sum_{j\neq 1} A_{ij} = -Kk_i^{\text{in}}$ for diagonal entries and $DF_{ij} \approx KA_{ij}$ for off-diagonal entries, i.e., $j \neq i$. A n oscillator j is part of the column control set if the sum of the off-diagonal entries in column j, $\sum_{i\neq j} KA_{il} = Kk_j^{\text{out}}$ is larger than the magnitude of the corresponding diagonal entry, Kk_j^{in}, or in other words, if the ratio of out-to-in degree is larger than one, i.e., $k_j^{\text{out}}/k_j^{\text{in}} > 1$. Thus, oscillators whose out-degree is larger than their in-degree will always be part of the column control set, i.e., the critical coupling value diverges, which we denote $K^*_{j,\text{col}} = \infty$ or $1/K^*_{j,\text{col}} = 0$. On the other hand, we expect that this trend generalizes so that oscillators with smaller out-to-in-degree ratios need little column control, i.e., have smaller critical coupling values K_{col}. In Fig. 5(a) we plot the inverse of the critical coupling value $1/K^*_{j,\text{col}}$ for each oscillator as a function of the degree ratio $k_j^{\text{out}}/k_j^{\text{in}}$ for the same network used in panel (a). The vertical dashed line indicates the ratio $k^{\text{out}}/k^{\text{in}} = 1$ beyond which we predict $1/K^*_{\text{col}}$ to vanish, and as expected, before this we find that the smaller this ratio, the smaller the value K^*_{col}. We note that this highlights two important properties of column control. First, it explains the plateau behavior observed in Fig. 3(a), (e) and (i), where the control fraction does not approach zero as coupling increases. Second, it suggests

TABLE 2. Numerical parameters values for the power grid model.

index, i	D_i	p_i	index, i	D_i	p_i
1	1.7476	-1.0697	21	0.7782	-0.1882
2	1.7524	-1.1012	22	0.4248	-0.1793
3	1.2024	-0.0432	23	0.4054	-0.1483
4	1.5625	-0.2034	24	0.2576	-0.1725
5	0.6620	-0.2707	25	0.8430	-1.0895
6	0.8039	-0.5232	26	1.7572	-1.1754
7	0.5685	-0.4292	27	1.6242	-0.6843
8	1.7742	-1.4545	28	1.1599	-1.1214
9	0.2117	-0.1619	29	0.8356	-0.6385
10	1.3095	-0.5943	30	0.2300	0.4905
11	0.8068	-0.3648	31	1.4356	2.3489
12	1.3422	-0.0851	32	1.3115	2.2129
13	0.4043	-0.2099	33	0.2642	0.3284
14	0.3241	-0.1242	34	1.3747	2.2736
15	1.1092	-0.8078	35	1.4981	2.8988
16	1.6324	-0.7955	36	0.3036	0.3549
17	1.1775	-1.0406	37	0.9786	1.5221
18	1.4898	-0.4910	38	1.7897	2.8252
19	0.2544	-0.2414	39	0.8235	1.4619
20	1.1897	-0.5919	–	–	–

that column control is likely very conservative and much less useful than row control in the strong coupling regime.

V. DISCUSSION

In conclusion, we have contributed to the understanding of reactive control in networks of heterogeneous phase oscillators, focusing on the dual strategy of row-column control. We have demonstrated that different network topologies can be controlled optimally depending on their structure, by directly targeting oscillators that are difficult to entrain (row), or by targeting oscillators with a strong influence on others (column). The particular role of each oscillator in the reactive control process is revealed by its algebraic contribution to the specific control strategy. These results have been shown to be applicable to real networks, and they pave the way for further studies on controlling power-grid and micro-grid networks. We speculate that this could even have applications in neuroscience, targeting specific brain areas to synchronize or desynchronize neural activity.

APPENDIX
PARAMETERS FOR THE IEEE 39 NEW ENGLAND POWER GRID EXAMPLE

Here we provide the numerical parameter choices for the power grid model presented in Fig. 2, namely, the damping coefficient, D_i, and power, p_i, for each oscillator in the network. Each oscillator $i = 1, \ldots, 39$ is was assigned a damping coefficient D_i and power p_i, summarized below. Note that damping coefficients were chosen uniformly at random from the interval [0.25,2.0] and power was chosen randomly from one or two normal distributions to ensure that power for loads and sources were biased negative and positive, respectively. Damping and power for each oscillator are given in Table 2.

REFERENCES

[1] S. H. Strogatz, *Sync: The Emerging Science of Spontaneous Order*. Glendale, CA, USA: Hypernion, 2003.

[2] A. Pikovsky, M. Rosenblum, and J. Kurths, *Synchronization: A Universal Concept in Nonlinear Sciences*. Cambridge, MA, USA: Cambridge Univ. Press, 2003.

[3] A. Arenas, A. Díaz-Guilera, J. Kurths, Y. Moreno, and C. Zhou, "Synchronization in complex networks," *Phys. Rep.*, vol. 469, pp. 93–153, 2008.

[4] A. Prindle, P. Samayoa, I. Razinkov, T. Danino, L. S. Tsimring, and J. Hasty, "A sensing array of radically coupled genetic 'biopixels'," *Nature*, vol. 481, pp. 39–42, 2012.

[5] L. Glass and M. C. Mackey, *From Clocks to Chaos: The Rhythms of Life*. Princeton, NJ, USA: Princeton Univ. Press, 1988.

[6] M. Rohen, A. Sorge, M. Timme, and D. Witthaut, "Self-organized synchronization in decentralized power grids," *Phys. Rev. Lett.*, vol. 109, 2012, Art. no. 064101.

[7] S. P. Cornelius, W. L. Kath, and A. E. Motter, "Realistic control of network dynamics," *Nat. Commun.*, vol. 4, 2012, Art. no. 1942.

[8] G. Yan, J. Ren, Y.-C. Lai, C.-H. Lai, and B. Li, "Controlling complex networks: How much energy is needed?," *Phys. Rev. Lett.*, vol. 108, 2012, Art. no. 218703.

[9] Y.-Y. Liu, J.-J. Slotine, and A.-L. Barabási, "Controllability of complex networks," *Nature*, vol. 473, pp. 167–173, 2011.

[10] Z. Yuan, C. Zhao, Z. Di, W.-X. Wang, and Y.-C. Lai, "Exact controllability of complex networks," *Nat. Commun.*, vol. 4, 2013, Art. no. 2447.

[11] J. Sun and A. E. Motter, "Controllability transition and nonlocality in network control," *Phys. Rev. Lett.*, vol. 110, 2013, Art. no. 208701.

[12] G. Menichetti, L. Dall'Asta, and G. Bianconi, "Network controllability is determined by the density of low in-degree and out-degree nodes," *Phys. Rev. Lett.*, vol. 113, 2014, Art. no. 078701.

[13] F. Pasqualetti, S. Zampieri, and F. Bullo, "Controllability metrics, limitations and algorithms for complex networks," *IEEE Trans. Control Netw. Syst.*, vol. 1, no. 1, pp. 40–52, Mar. 2014.

[14] T. Menara, D. S. Bassett, and F. Pasqualetti, "Structural controllability of symmetric networks," *IEEE Trans. Autom. Control*, vol. 4, no. 9, pp. 3740–3747, Sep. 2019.

[15] A. N. Montanari, C. Duan, L. A. Aguirre, and A. E. Motter, "Functional observability and target state estimation in large-scale networks," *Proc. Natl. Acad. Sci.*, vol. 119, 2022, Art. no. e2113750119.

[16] C. Duan, T. Nishikawa, and A. E. Motter, "Prevalence and scalable control of localized networks," *Proc. Natl. Acad. Sci.*, vol. 119, 2022, Art. no. e2122566119.

[17] F. C. Hoppensteadt and E. M. Izhikevich, "Oscillatory neurocomputers with dynamic connectivity," *Phys. Rev. Lett.*, vol. 82, 1999, Art. no. 2983.

[18] P. S. Skardal, D. Taylor, and J. Sun, "Optimal synchronization of complex networks," *Phys. Rev. Lett.*, vol. 113, 2014, Art. no. 144101.

[19] M. Fazlyab, F. Dórfler, and V. M. Preciado, "Optimal network design for synchronization of coupled oscillators," *Automatica*, vol. 84, pp. 181–189, 2017.

[20] A. Forrow, F. G. Woodhouse, and J. Dunkel, "Functional control of network dynamics using designed laplacian spectra," *Phys. Rev. X*, vol. 8, 2018, Art. no. 041043.

[21] T. Menara, G. Baggio, D. S. Bassett, and F. A. Pasqualetti, "A framework to control functional connectivity in the human brain," in *Proc. IEEE Conf. Decis. Control*, 2019, pp. 4697–4704.
[22] G. Baggio, D. S. Bassett, and F. Pasqualetti, "Data-driven control of complex networks," *Nat. Commun.*, vol. 12, 2021, Art. no. 1429.
[23] T. Menara, G. Baggio, D. S. Bassett, and F. Pasqualetti, "Functional control of oscillator networks," *Nat. Commun.*, vol. 13, 2022, Art. no. 4721.
[24] R. O. Grigoriev, M. C. Cross, and H. G. Schuster, "Pinning control of spatiotemporal chaos," *Phys. Rev. Lett.*, vol. 79, 1997, Art. no. 2795.
[25] X. F. Wang and G. Chen, "Pinning control of scale-free dynamical networks," *Phys. Appl.*, vol. 310, pp. 521–531, 2002.
[26] X. Li, X. F. Wang, and G. Chen, "Pinning a complex dynamical network to its equilibrium," *IEEE Trans. Circuits Syst. I: Fundam. Theory Appl.*, vol. 51, no. 10, pp. 2074–2087, Oct. 2004.
[27] P. S. Skardal and A. Arenas, "Control of coupled oscillator networks with application to microgrid technologies," *Sci. Adv.*, vol. 1, 2015, Art. no. e1500339.
[28] Y. Kuramoto, *Chemical Oscillations, Waves, and Turbulence*. New York, NY, USA: Springer, 1984.
[29] A. Ben-Israel and T. N. E. Grenville, *Generalized Inverses*. New York, NY, USA: Springer, 1974.
[30] P. S. Skardal, D. Taylor, and J. Sun, "Optimal synchronization of directed complex networks," *Chaos*, vol. 26, 2016, Art. no. 094807.
[31] P. S. Skardal, D. Taylor, J. Sun, and A. Arenas, "Collective frequency variation in network synchronization and reverse PageRank," *Phys. Rev. E.*, vol. 93, 2016, Art. no. 042314.
[32] G. H. Golub and C. F. Van Loan, *Matrix Computations*. Baltimore, MD, USA:Johns Hopkins Univ. Press, 1996.
[33] A. Békéssy, P. Bekessy, and J. Komlós, "Asymptotic enumeration of regular matrices," *Stud. Sci. Math. Hung.*, vol. 7, pp. 343–353, 1972.
[34] T. Athay, R. Podmore, and S. Virmani, "A practical method for the direct analysis of transient stability," *IEEE Trans. Power App. Syst.*, vol. 2, no. 2, pp. 573–584, Mar. 1979.
[35] C. Grigg et al., "The IEEE reliability test System-1996. a report prepared by the reliability test system task force of the application of probability methods subcommittee," *IEEE Trans. Power Syst.*, vol. 14, no. 3, pp. 1010–1020, Aug. 1999.
[36] F. Dórfler and F. Bullo, "Synchronization and transient stability in power networks and nonuniform kuramoto oscillators," *SIAM J. Control Optim.*, vol. 50, pp. 1616–1642, 2012.
[37] J. W. Simpson-Porco, F. D'orfler, and F. Bullo, "Synchronization and power sharing for droop-controlled inverters in islanded microgrids," *Automatica*, vol. 49, pp. 2603–2611, 2013.
[38] F. Dórfler, M. Chertkov, and F. Bullo, "Synchronization in complex oscillator networks and smart grids," *Proc. Nat. Acad. Sci.*, vol. 110, pp. 2005–2010, 2013.
[39] T. Nishikawa and A. E. Motter, "Comparative analysis of existing models for power-grid synchronization," *New J. Phys.*, vol. 17, 2015, Art. no. 015012.

PER SEBASTIAN SKARDAL received the B.A. degree in mathematics from Boston College, Newton, MA, USA, in 2008, and the M.S. and Ph.D. degrees in applied mathematics from the University of Colorado Boulder, Boulder, CO, USA, in 2010 and 2013, respectively. From 2013 to 2015, he was a Postdoctoral Scholar with Universitat Rovira i Virgili, Tarragona, Spain. He is currently an Associate Professor of mathematics with Trinity College, Hartford, CT, USA.

ALEX ARENAS received the Ph.D. degree in physical sciences from the University of Barcelona, Barcelona, Spain, in 1996. He is currently a Professor of computer engineering and mathematics with Universitat Rovira i Virgili, Tarragona, Spain, External Faculty with Complexity Science Hub, Vienna, Austria, and Chief Scientist of complex systems science with Pacific Northwest National Laboratory, Richland, WA, USA. His scientific career has focused on the study of complex network systems. He is the Editor of Interdisciplinary Physics section, *Physical Review E*, *Journal of Complex Networks*, and *Journal of Computational Social Science*. He is a Fellow of the American Physical Society (2018) and the Network Science Society (2020). He was the recipient of the Mathematics and Society Award of the Ferran Sunyer i Balaguer Foundation in 2020, ICREA Academia in 2011 and 2017, Scientific Award recognition, Ciutat de Tarragona in 2022, and Narcís Monturiol Medal to Scientific Merit in 2022.